Molecules and Cells

PPARα-Target Gene Expression Requires TIS21/BTG2 Gene in Liver of the C57BL/6 Mice under Fasting Condition

Allen Eugene Hong[1,6], Min Sook Ryu[2,6], Seung Jun Kim[3], Seung Yong Hwang[3,4], and In Kyoung Lim[1,2,5,*]

[1]Ajou Graduate School of medicine, Suwon 16499, Republic of Korea, [2]BK Plus program, Department of Biomedical Sciences, Ajou University Graduate School of Medicine, Suwon 16499, Korea, [3]R&D center, BioCore Co. Ltd., Seoul 08511, Korea, [4]Department of Bio-Nanotechnology, Hanyang University, Ansan 15588, Korea [5]Department of Biochemistry and Molecular Biology, Ajou University School of Medicine, Suwon 16499, Korea, [6]These authors contributed equally to this work.
*Correspondence: iklim@ajou.ac.kr
http://dx.doi.org/10.14348/molcells.2018.2257
www.molcells.org

The TIS21/BTG2/PC3 gene belongs to the antiproliferative gene (APRO) family and exhibits tumor suppressive activity. However, here we report that TIS21 controls lipid metabolism, rather than cell proliferation, under fasting condition. Using microarray analysis, whole gene expression changes were investigated in liver of TIS21 knockout (TIS21-KO) mice after 20 h fasting and compared with wild type (WT). Peroxisome proliferator-activated receptor alpha (PPARα) target gene expression was almost absent in contrast to increased lipid synthesis in the TIS21-KO mice compared to WT mice. Immunohistochemistry with hematoxylin and eosin staining revealed that lipid deposition was focal in the TIS21-KO liver as opposed to the diffuse and homogeneous pattern in the WT liver after 24 h starvation. In addition, cathepsin E expression was over 10 times higher in the TIS21-KO liver than that in the WT, as opposed to the significant reduction of thioltransferase in both adult and fetal livers. At present, we cannot account for the role of cathepsin E. However, downregulation of glutaredoxin 2 thioltransferase expression might affect hypoxic damage in the TIS21-KO liver. We suggest that the TIS21/BTG2 gene might be essential to maintain energy metabolism and reducing power in the liver under fasting condition.

Keywords: BTG2, fatty acid oxidation, liver metabolism, PPARα, starvation

INTRODUCTION

During starvation, nutrient metabolism should adapt in order to preserve life in the absence of caloric intake. The initial response to fasting is hormonal regulation (e.g. glucagon, catecholamine) to maintain the blood glucose level. Soon thereafter, the glucose insufficiency triggers catabolic reactions such as breakdown of glycogen stored in liver and muscle, fat from adipose tissue, and amino acid from skeletal muscle. As a result, fatty acids are released into the systemic circulation to feed peripheral tissues and liver. Liver assimilates fatty acids and generates ketone bodies, which covers two-thirds of the caloric requirement of the brain during the period of fasting (Cahill Jr, 2006). Overall, anabolic reactions regulated by insulin signaling are shifted to catabolism (e.g. fatty acid oxidization in mitochondria and peroxisomes).

The fatty acid oxidation and ketone body producing enzymes in the liver are induced mainly by peroxisome proliferator-activated receptor alpha (PPARα) (Rakhshandehroo et

Received 15 October, 2017; revised 18 December, 2017; accepted 20 December, 2017; published online 29 January, 2018

eISSN: 0219-1032

al., 2010), while fatty acid/sterol synthetic enzymes regulated by sterol regulatory element-binding transcription factor (SREBF)1c and SREBF2 are all reduced during fasting (Hakvoort et al., 2011; Schupp et al., 2013; Zhang et al., 2011). As lipid oxidation requires many oxido-reductive enzymes, the cytochrome P450 family enzymes and antioxidant proteins are also induced during starvation. Along with these fasting responses, *Tis21*/*Btg2*/*Pc3* is induced in liver, muscle, and adipose tissues in mouse models in response to starvation (Kim et al., 2014; Schupp et al., 2013).

TPA-Inducible Sequence 21 (TIS21) has been reported as one of the primary response genes induced by the tumor promoter, 12-*O*-tetradecanoylphorbol-13-acetate (TPA), in mice (Fletcher et al., 1991). TIS21 expression is differential in mouse thymic carcinoma tissues and human lung cancer cells compared with those of the normal tissues (Lim et al., 1995), suggesting its role as a potential tumor suppressor in the thymus and lung. B-cell translocation gene 2 (BTG2) and PC3 are ortholog genes of TIS21 in human, and rat, respectively (Bradbury et al., 1991; Rouault et al., 1996), that regulates cell proliferation, apoptosis and cellular senescence in p53-dependent and -independent manners (Lim, 2006). Loss of BTG2 expression has been reported in various tumors (e.g. prostate, kidney, and breast) and its anti-carcinogenic mechanisms are evidenced in *in vivo* knockout mice and *in vitro* cell culture analyses (Choi et al., 2016; Lim, 2006; Mao et al., 2015; Park et al., 2008).

Recent reports suggested that TIS21 activates gluconeogenesis. The overexpression of BTG2 in AML-12 immortalized mouse liver cells increases glucose output by inducing the transcription of gluconeogenic genes. The same study documented the same results in a mouse model (Hwang et al., 2012; Kim et al., 2014). However, there no study has addressed the regulation mechanism of lipid metabolism by the TIS21 gene under fasting condition.

In this paper, we report the regulation of lipid metabolism by the TIS21 gene using the TIS21-knockout (TIS21-KO) mouse model by employing microarray analysis. The fatty acid oxidation and synthesis pathways were significantly affected in the TIS21-KO mice.

MATERIALS AND METHODS

Animal

All mice used for the present study were maintained under the SPF condition at the Ajou University Animal Care Center under constant temperature and constant humidity with light/dark cycle 12/12 h, starting at 7 o'clock in the morning. WT and TIS21-KO mice were generated previously in the C57BL/6 background (Park et al., 2004). All mice were maintained *ad libitum* before fasting experiment for the indicated duration (20-48 h). All of the animal procedures were followed by Ajou University Institutional Review Board.

Microarray & data processing

Total cellular RNAs were extracted from livers of the WT and TIS21-KO adult male mice (10 week-old, male) and fetal livers of the 13.5 day-old embryos using TRIzol (Invitrogen, USA). To minimize variation of metabolism and to synchronize metabolic status in the mice, all mice were fasted for 20 h (from 5:00 pm to next day 1:00 pm), and the fetal livers derived from female mice ($n > 3$) were pooled before RNA extraction. These samples were processed and hybridized on Agilent SurePrint G3 Mouse GE 8X 60K array covered by the Gasket 8-plex slide (Agilent technologies, USA), then data were processed and analyzed using GeneSpring GX12.6 (Agilent technologies, USA). The methods and data processing procedures are described elsewhere (Lee et al., 2012), and raw data is available on NCBI's Gene Expression Omnibus (GEO) as GSE105772.

Data analysis

After selecting the differentially expressed genes (DEGs; ± 1.5 fold, $p < 0.05$) between the TIS21-KO *vs.* WT mice, the data was analyzed by DAVID functional annotation tool to find out highly enriched gene ontologies (GOs) (Huang et al., 2008; 2009). The whole DEGs were listed in Table 1, and arbitrarily segmented based on their transcription amplitudes (Table 2). In addition, the relative expression folds were analyzed by performing Gene Set Enrichment Analysis (GSEA) (Mootha et al., 2003; Subramanian et al., 2005). To search the upstream transcription factors for the DEGs, enriched transcription factor binding site (TFBS) of the affected genes were queried to DAVID functional annotation based on the UCSC-TFBS database. The metabolic pathways were illustrated by Cytoscape 3.2.1 based on KEGG pathways (Kanehisa and Goto, 2000; Kanehisa et al., 2016; Shannon et al., 2003).

RNA extraction and Real-time quantitative PCR

Total cellular RNAs were isolated with RNAiso plus™ (Takara, Japan) according to the manufacturer's instruction. Then 1.0 μg of total RNAs were reverse-transcribed with Oligo(dT)$_{18}$ by using PrimeScript reverse transcriptase (Takara, Japan), and the cDNAs were amplified with 2X qPCR mix (Nanohelix, South Korea). qPCR reactions were performed by CFX96 Touch™ Real-Time PCR Detection System (BioRad, USA). Sequences of the primer sets are listed on the Supplementary Table S1.

Quantification of triglyceride and cholesterol contents in liver

Lipid contents were extracted according the method described (Folch et al., 1957; Newberry et al., 2003); liver homogenates isolated from the 10 week old male mice were prepared in 10 volumes of 1x PBS by using Dounce homogenizer, and protein concentrations were determined by Bradford method. The homogenates (300 μl) were added to the mixture of chloroform-methanol (2:1 v/v, 5 ml) plus 0.1% sulfuric acid (0.5 ml), and then incubated with agitation for ~2 h at room temperature. The organic phase was dried by SpeedVac under low vacuum. Extracted lipids were re-suspended in 1x PBS (300 μl) with 2% Triton X-100, and the triglyceride and cholesterol levels were measured by colorimetric assay in the Ajou University Hospital. Final contents were normalized based on the protein concentration of the initial homogenates.

Statistical analysis

Data were analyzed with two-sided Student *t*-test, and the p-values < 0.05 were considered as significant between the two comparing groups.

RESULTS

TIS21 gene knockout changes metabolic profiles in mouse liver after fasting stimulation

To investigate any effect of TIS21 on nutrient metabolism, TIS21-KO and wild type (WT) male mice were fasted for 20 h before sacrifice and the gene expression profiles were evaluated by microarray analysis. Furthermore, 13.5 day old embryos were evacuated from the womb to examine the activity of the TIS21 gene in the fetal stage. mRNAs isolated from livers of the 'KO-adult', 'WT-adult', 'KO-fetus', and 'WT-fetus' were screened, and the effects of the TIS21 gene after 20 h of fasting were compared with that of the WT, *e.g.* KO-adult *vs.* WT-adult, and KO-fetus *vs.* WT-fetus (Fig. 1A). Among the 55,681 probes provided by the microarray chip, 26,988 probes were positive at least in one group. By applying a cutoff threshold ± 2-fold with $p < 0.05$ difference, 1,109 genes and 280 genes were differentially expressed in the KO-adult and the KO-fetus, respectively. Expression of hepatic *Tis21* mRNA was 6 times higher in the fetal stage than the adult stage (Supplementary Fig. S1A), which is consistent with a previous report of observations using *in situ* hybridization of whole embryos (Lim, 2006). Other adult- or fetal-stage selective genes (> ±10 times in adult/fetus) were 98.2% identical between WT and TIS21-KO mice (Supplementary Fig. S1B). Among those, 90% of the genes were positively-correlated and 8.2% were negatively-correlated with the reference gene set reported previously (Li et al., 2012).

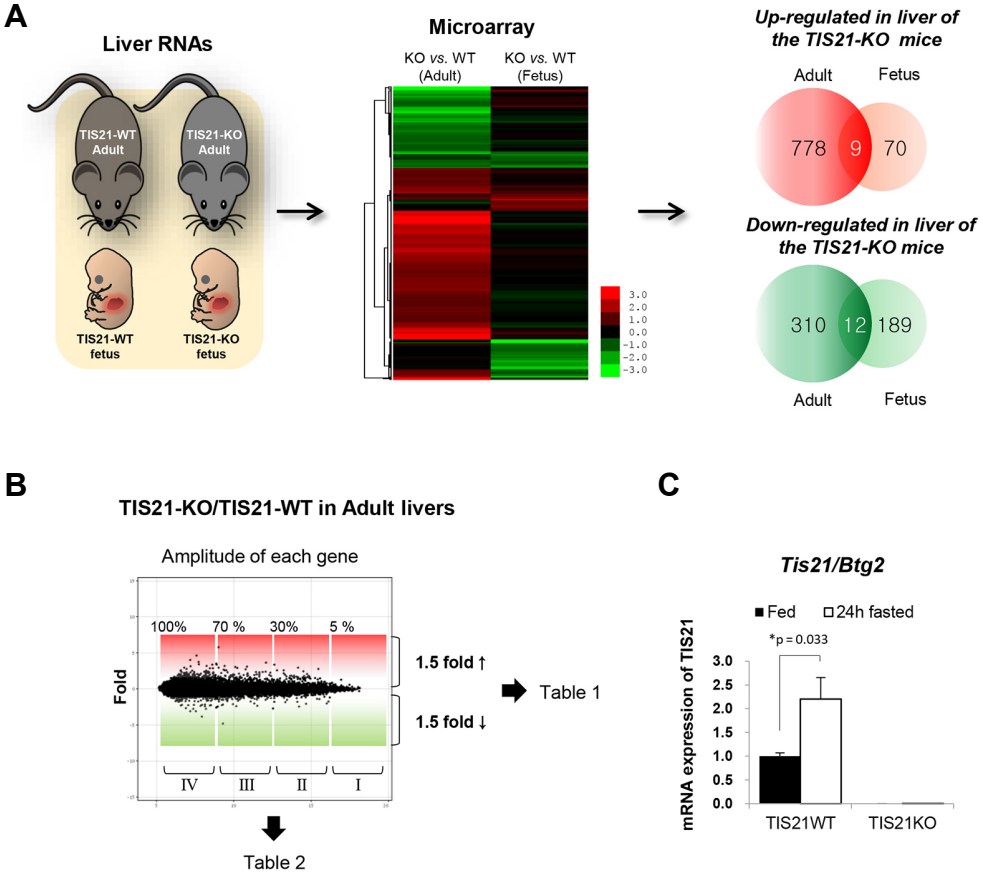

Fig. 1. Starvation-regulated gene expression profile in livers of the TIS21-KO mice analyzed by Agilent gene chips. (A) Total cellular RNAs were isolated from liver of the 10-week old male mice after 20 h starvation and the 13.5 day-old fetus of the C57BL/6 mice with (TIS21-WT) and without (TIS21-KO) TIS21$^{/BTG2}$ gene. The mRNAs were purified before analysis with Agilent gene chips. Gene expression profile obtained from the KO mice livers were presented as the relative values based on those of the WT. Venn diagram comparing significantly regulated genes ($p < 0.05$, ± 2 fold changes). (B) M (log ratio) *vs.* A (mean average) plot represents each gene as a dot with its relative expression fold (TIS21-KO/TIS21-WT) on Y-axis, and amplitude of the gene (= 1/2 x $\log_2$ [TIS21-WT x TIS21-KO]) on X-axis. Differentially expressed genes (DEGs) selected by the fold are summarized in the Table 1, and the DEGs with different amplitudes were presented in the Table 2. (C) RT-qPCR analysis showing TIS21 expression in liver of C57BL/6 mice normalized by β-actin. ($n = 3$ per fed group, and $n = 6$-8 per 24 h fasting group)

When we evaluated the differentially expressed genes (DEGs) between the WT and TIS21-KO mice using the DAVID web-based program with a less stringent criterion (over ±1.5-fold, KO/WT with $p < 0.05$), 1,680 genes were upregulated and 1,006 genes were downregulated in adult mice livers (Fig. 1B). The expression of *Tis21* was significantly increased after 20 h fasting in adult mice (Fig. 1C), suggesting that TIS21 gene may have a role in liver of mice in response to fasting stimulation.

Metabolism-regulating genes require TIS21 expression under fasting condition

To further investigate effect of TIS21-KO under fasting condition, the DEGs were analyzed by DAVID and the GO terms are listed in Table 1. In the biological process, metabolism of xenobiotics by cytochrome P450, immune response, and steroid biosynthetic process were prominent, and microsome and lysosome component was upregulated, and glutathione transferase activity was high in the molecular function. On the other hand, genes in the PPAR signaling pathway and fatty acid metabolism were significantly reduced in the TIS21-KO than the WT in response to fasting stimulation (Fig. 1B, Table 1). When the DEGs were ranked based on the amplitude of each gene expression from the highest to the lowest, the top 5% of the genes were clustered in the metabolism of xenobiotics and fatty acyl metabolic process (Fig. 1B, Table 2). The top 30% of the genes in the middle rank exhibited immune response regulation, such as antigen processing and presentation along with complement and coagulation cascades. Genes regulating cell division cycle and signaling pathways were expressed much less. Although the intensity of an mRNA transcript does not always directly reflect its protein level, our data was enough to assume a major role of TIS21 gene in the liver under starvation. The

Table 1. Gene ontology terms of the differentially expressed genes observed from livers of the TIS21-KO mice compared with those of the WT in adult stage

	GO term	Enrichment score	Genes Count	*p*-value
Significantly increased in the TIS21-KO *vs.* WT mice	Biological process			
	Metabolism of xenobiotics by cytochrome P450	10.0	32	2.1E-16
	Immune response	9.2	93	8.8E-19
	Steroid biosynthetic process	8.1	30	2.9E-15
	Antigen processing and presentation of peptide antigen	5.6	19	4.4E-12
	Regulation of phagocytosis	4.0	12	5.3E-07
	Response to bacterium	3.8	27	7.1E-05
	Cellular component			
	Microsome	8.6	42	8.8E-11
	Lysosome	4.6	34	1.8E-06
	Molecular function			
	Glutathione transferase activity	4.6	12	8.6E-07
	Steroid dehydrogenase activity, acting on the CH-OH group of donors, NAD or NADP as acceptor	4.3	11	2.0E-06
Significantly decreased in the TIS21-KO *vs.* WT mice	Biological process			
	PPAR signaling pathway	5.7	17	3.1E-07
	Acyl-CoA metabolic process	3.4	9	3.9E-07
	Polyol metabolic process	2.8	8	1.2E-03
	Fatty acid metabolism	2.0	12	3.3E-06
	Cellular component			
	Peroxisome	3.8	18	1.9E-07
	Microsome	2.2	16	1.9E-03
	Mitochondrial part	2.0	32	5.3E-03
	Organelle membrane	1.9	50	2.9E-04
	Molecular function			
	Cofactor binding	4.5	27	1.2E-06
	Nucleotide binding	2.3	118	3.6E-04

Enriched gene ontology terms (GO) among the differentially expressed genes (DEGs) were analyzed by DAVID web-based program (https://david.ncifcrf.gov/). Upon selection of DEGs at cutoff as ±1.5-fold with $p<0.05$, significantly increased and significantly decreased genes were counted as 1680, and 1006, respectively. GO terms with Top 10 were enlisted.

Table 2. Gene ontology analysis of the differentially expressed genes, based on the amplitudes of the genes

Rank (from top)	GO term	Clustered gene count (Up/Down)
Ⅰ (~5%)	Metabolism of xenobiotics by cytochrome P450	9 (9/0)
	Fatty acid degradation	13 (2/11)
	Arachidonic acid metabolism	7 (3/4)
	Endoplasmic reticulum	36 (28/8)
	Heme binding	16 (12/4)
Ⅱ (5~30%)	Metabolism of xenobiotics by cytochrome P450	13 (11/2)
	Steroid biosynthetic process	16 (13/3)
	Antigen processing and presentation	7 (7/0)
	Complement and coagulation cascades	11 (11/0)
	Heme binding	19 (15/4)
Ⅲ (30~70%)	Cholesterol metabolic process	12 (12/0)
	Iron ion homeostasis	8 (6/2)
	Integrin-mediated signaling pathway	11 (10/1)
	B cell receptor signaling pathway	10 (8/2)
	Cyclin-dependent protein kinase complex	6 (5/1)
Ⅳ (70~100%)	Cell cycle	41 (36/5)
	Protein phosphorylation	35 (31/4)
	Toll-like receptor signaling pathway	5 (5/0)
	Carbohydrate metabolic process	11 (9/2)
	Renin-angiotensin system	6 (6/0)

Metabolism-related, Immune-related, Cell cycle/Signaling-related

collective data strongly suggest that xenobiotic metabolism and fatty acid oxidation might require TIS21 gene expression under starved condition.

PPARα-target gene expression is reduced in the TIS21-KO mice under fasting

To investigate the metabolic pathways that are significantly changed in the TIS21-KO mice under fasting condition, the DEGs were further analyzed by gene set enrichment analysis (GSEA) and UCSC-TFBS analysis. As shown in Figs. 2A and 2B, gene expression under SREBF1/2 was significantly increased, as opposed to lack of the genes regulated by PPARα in the TIS21-KO mice (Supplementary Fig. S2). Indeed, expression of *Fasn*, *Scd1*, and *Scd2* regulating fatty acid synthesis was significantly increased, in contrast, fatty acid oxidation genes in mitochondria and peroxisome were clearly downregulated in KO mice. Overall metabolic process observed in liver of the TIS21-KO mice are depicted in Fig. 2C, which show increased SREBF1/2 targets and reduced PPARa target gene expression. The scheme also revealed that glucose metabolic pathway such as glycolysis/gluconeogenesis or tricarboxylic acid cycle, were unaffected in the TIS21-KO liver with 20 h fasting. The DEG changes between the KO and WT were validated by RT-qPCR analyses (Figs. 2D-2E). When the promoters of DEGs were examined by the UCSC-TFBS analysis, PPARα was the most frequently observed transcription factor interacting with promoters of the DEGs, followed by STAT5B and NF-κB (Table 3, with selections from the transcription factors shown in Supplementary Fig. S3). The observations were the same in both adult and fetal livers. In summary, TIS21-KO liver increased the expression of fatty acid/cholesterol synthesis enzymes (SREBF1/2 targets), whereas fatty acid degrading enzymes (PPARα targets) were significantly reduced in the TIS21-KO liver compared to those of the WT under fasting condition.

Starvation-induced fatty change is diffuse in WT liver, but focal in TIS21-KO mice

When the fat deposition in liver was evaluated by Oil red O staining, 24 h fasting significantly increased lipid deposition in the livers of both WT and TIS21-KO mice compared to those of non-fasted mice (Fig. 3A), and the fatty change was accompanied by the increase of triglyceride (TG) and cholesterol after 24 h fasting (Fig. 3E). However, the increase was not significantly different between the WT and TIS21-KO mice. Immunohistochemisty analysis by hematoxylin and eosin staining revealed that 24 h fasting significantly induced microvesicular fatty change in both male and female WT mice (Figs. 3C and 3D). The fat distribution was diffuse and homogeneous in the WT, whereas it was focal in TIS21-KO liver at the centrilobular zone of both male and female mice (Supplementary Table S2 and Supplementary Fig. S4A). Oil red O staining in female liver showed that lipid deposition was more severe in the TIS21-KO mice than that of the WT

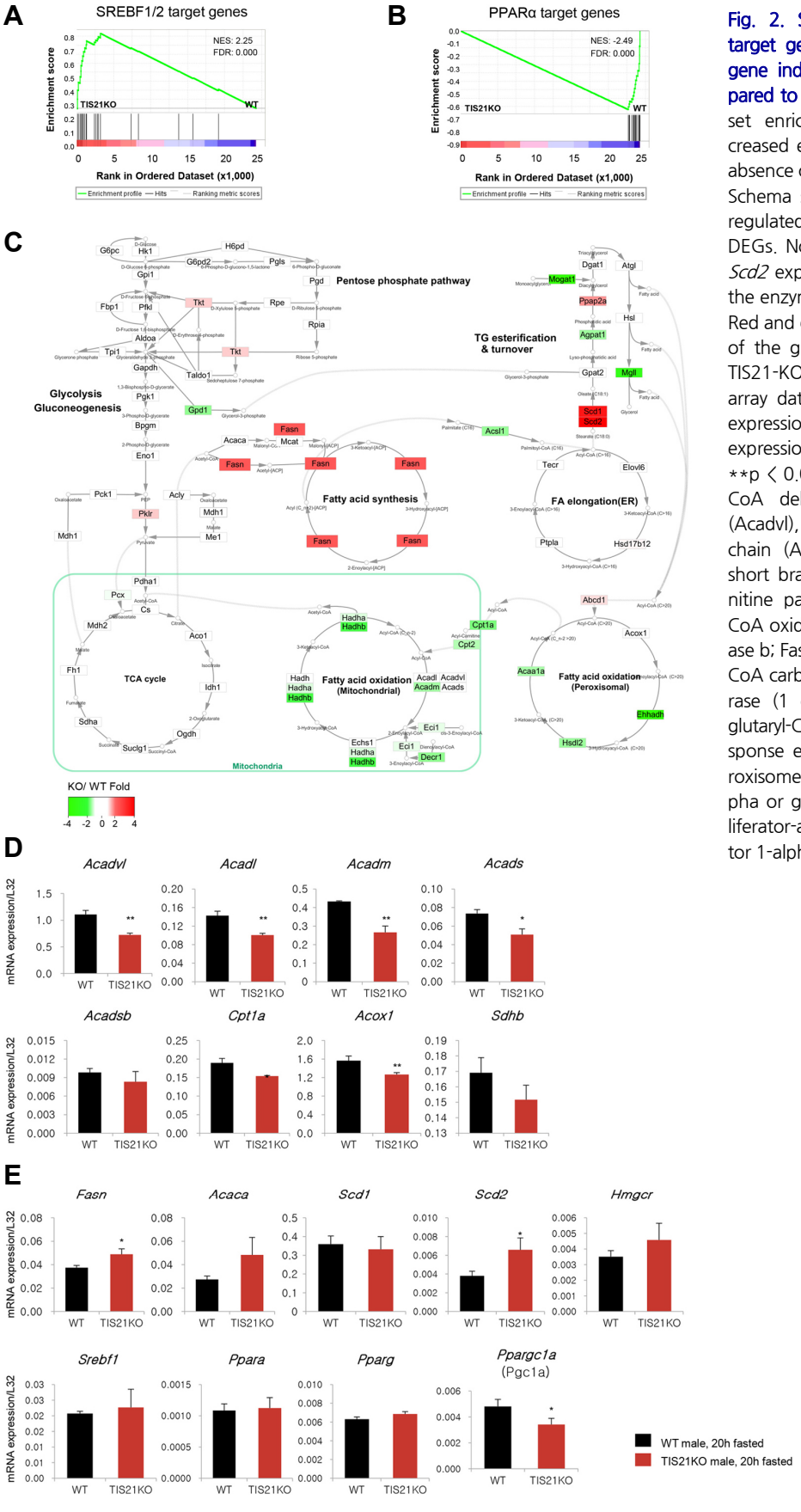

Fig. 2. Significant expression of SREBF1/2 target genes, but absence of PPARα target gene induction in the TIS21-KO mice compared to those of the wild type. (A, B) Gene set enrichment analyses showing the increased expression of SREBF1/2 targets, but absence of PPARα target gene expression. (C) Schema showing the biochemical pathways regulated in the TIS21-KO livers based on the DEGs. Note significant increase of *Fasn* and *Scd2* expression as opposed to reduction of the enzymes regulating fatty acid catabolism. Red and green indicate increase and decrease of the gene expression, respectively, in the TIS21-KO liver. (D, E) Validation of the microarray data by RT-qPCR. PPARα target gene expression (D) and SREBF1/2 target gene expression (E) were presented. *p < 0.05, **p < 0.01 between KO *vs.* WT. Acad: acyl-CoA dehydrogenase of very long chain (Acadvl), of long chain (Acadl), of medium chain (Acadm), of short chain Acads), of short branched chain (Acadsb); Cpt1a, carnitine palmitoyltransferase 1a; Acox1, acyl-CoA oxidase 1; Sdhb, succinate dehydrogenase b; Fasn, fatty acid synthase; Acaca, acetyl-CoA carboxylase a, Scd, stearoyl-CoA desaturase (1 or 2); Hmgcr, 3-hydroxy-3-methyl-glutaryl-CoA reductase; Srebf1, steroid response element binding factor 1; Ppar, peroxisome proliferator-activated receptor (alpha or gamma); Ppargc1a, peroxisome proliferator-activated receptor gamma coactivator 1-alpha.

Table 3. Frequently found transcription factors that binds to the promoters of the DEGs in livers of the TIS21-KO *vs.* TIS21-WT mice

TIS21-KO vs. TIS21-WT			
Adult mice		Fetus	
Upregulated genes (748)	Downregulated genes (401)	Upregulated genes (164)	Downregulated genes (263)
PPARα (363)	PPARα (152)	PPARα (54)	PPARα (108)
STAT5B (235)	STAT5B (95)	STAT5B (35)	STAT5B (74)
NFκB (257)	NFκB (93)		NFκB (71)
	STAT3 (127)		STAT3 (96)

( )Counts of genes that contain the denoted transcription factor binding site on their promoters.

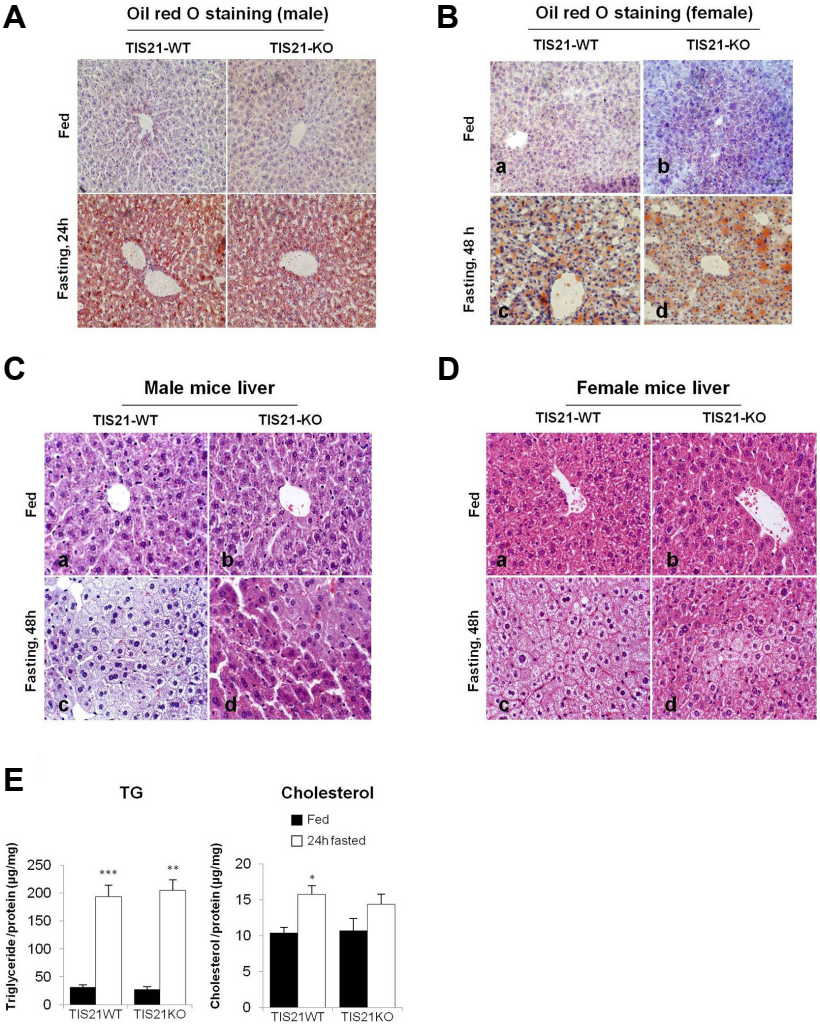

Fig. 3. Histologic changes in the TIS21-KO liver compared with that of the WT in response to starvation. (A) Oil red O staining in male mice liver: Twenty four hour-fasting significantly increased fat contents in liver of both KO and WT mice, compared with those of the fed condition. However, there was no significant difference between the KO and WT. (B) Oil red O staining of female liver: Under fed condition, fat deposition is more in the KO than the WT, whereas 48 h-starvation significantly increased fat contents in both KO and WT mice. (C) Differential effect of TIS21 gene knockout on fat mobilization in liver of male mice after 48 h fasting: Micro-vesicular fatty change was severe in the WT than that in the KO in response to starvation (compare (c) and (d) panels in Fig 3C), however, centri-lobular fat deposition was more severe in the KO than the WT under starvation condition. In fed condition, there was no specific difference between the WT and KO. (D) Differential effect of TIS21 gene knockout on fat mobilization in liver of female mice after 48 h fasting: Micro-vesicular fatty change was more severe in the WT than that in the KO after starvation. On the other hand, centri-lobular focal fat distribution was clear in the KO than the WT under starvation condition. (Compare (c) and (d) panels in Fig. 3D). (E) 24h-fasting significantly increased Triglyceride (TG) and cholesterol level in both WT and KO mice, whereas it was not significantly different between the WT and KO in response to 24h-fasting. Number of the mice used for WT-fed, WT-fasted, KO-fed, KO-fasted are 4,8,2,6, respectively. $*p < 0.05$, $**p < 0.01$, $***p < 0.0001$ between fed and fasted.

under fed condition (compare *a* and *b* panels, Fig. 3B). We speculate that fasting-induced uneven or patchy like change and whitish mottling in the liver (Supplementary Fig. S4B) may reflect the focal fat deposition in TIS21-KO mice at the centrilobular area (Supplementary Table S2). In summary, there was no pathologic change in liver of TIS21-KO mice, except starvation-induced focal fat distribution described above.

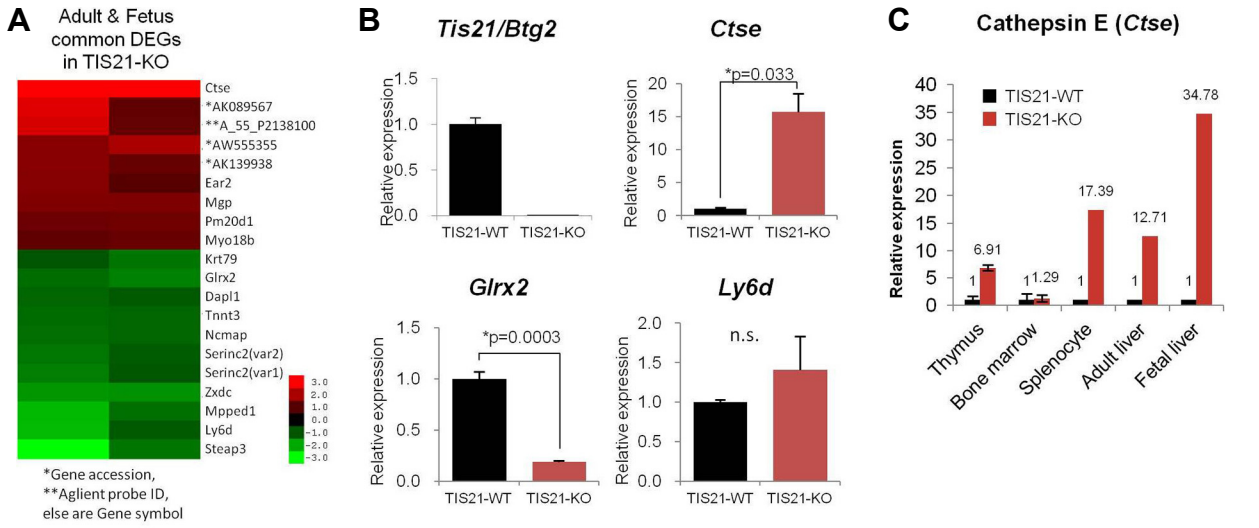

Fig. 4. Induction of cathepsin E expression but reduced glutaredoxin 2 in liver of the TIS21-KO mice in both adult and fetus. (A) Heatmap of common DEGs found in the adult and fetal livers of TIS21KO mice. Raw data is displayed in the Supplementary Table S3. (B) RT-qPCR analysis of liver: RNAs were isolated from the 10 week old male mice without fasting and then subjected to the analysis ($n = 3$ per each group). Note significant increase of cathepsin E (Ctse) as opposed to significant decrease of glutaredoxin 2 (Glrx2) expression in KO livers than those in the WT. Lymphocyte antigen 6 days (Ly6d) expression was also measured, but not significantly different. The data is accordant with that of the cDNA analysis. (C) Cathepsin E expression is increased not only in adult liver but also in other lymphoid organs, such as thymus and splenocytes.

Cathepsin E expression is highest in the DEGs of adult and fetal livers in TIS21-KO mice

To figure out the effect of TIS21 gene knockout on liver development, the DEGs (KO *vs.* WT) obtained from both adult and fetal livers were examined and then selected the commonly increased 9 genes and the decreased 12 genes in the TIS21-KO mice compared to the WT were determined (Figs. 1A and 4A). Using RT-qPCR, the highest expression of cathepsin E (*Ctse*) and the lowest expression of glutaredoxin 2 (*Glrx2*) were proven in the TIS21-KO mice compared to WT mice (Fig. 4B and Supplementary Table S3). Expression of cathepsin E was significantly increased not only in the adult and fetal livers but also in other lymphoid organs, such as thymus and mature splenocytes (Fig. 4C).

DISCUSSION

In the present study, the effect of TIS21 gene on energy metabolism has been investigated using microarray analysis in adult and fetal livers dissected from the whole body of TIS21-KO mice after overnight fasting stimulation. The liver was the focus of study because it is the center of metabolism and since TIS21 is highly expressed in fetal liver (Lim, 2006; Terra et al., 2008). By analyzing gene ontology terms, we found that TIS21-KO significantly increased xenobiotic metabolism by cytochrome P450 and immune response rather than the regulation of cell division cycle after overnight fasting (Tables 1 and 2). In addition, the PPARα signaling pathway and fatty acid catabolism were significantly inhibited in the TIS21-KO mice compared to those of the WT mice (Fig. 2, Table 3). GSEA revealed that fatty acid/steroid synthesis and fatty acid oxidation were inversely regulated in the TIS21-KO mice compared with WT mice under fasting condition. Increased Oil-red O staining in the female KO mice (Fig. 3B) might be concordant with the GSEA data shown in Fig. 2A. The data strongly suggests that TIS21 might be essential in energy metabolism upon starvation by regulating lipid metabolism.

Starvation stimulates autophagy in the liver (Komatsu et al., 2005; Mizushima et al., 2004; Rabinowitz and White, 2010), and the response requires nutrient sensing nuclear receptors such as PPARα (Lee et al., 2014) Hence, the suppression of PPARα pathway in TIS21-KO mice can be linked to suppression of the autophagy reaction. We previously described that mechanistic target of rapamycin (mTOR) signaling is constitutively activated in TIS21KO-mouse embryonal fibroblasts in response to estradiol (Kim et al., 2008). Therefore, we speculate that the autophagy reaction can be reduced in liver of TIS21-KO mice under fasting condition. In C57BL/6 mice, 24 h-fasting significantly reduced body weight (13%) compared to that of mice that were fed, and the weight loss was larger in WT mice than in KO mice. The smaller weight loss under the starvation condition was also evident in the weight of organs such as the liver and gonadal white adipose tissues, of the KO mice than the WT mice (Supplementary Fig. S5). This observation indirectly supports the failure of autophagy and lipid catabolism in the TIS21-KO mice compared to the WT. In the TIS21-KO mice, compromised lipid catabolism may lead to failure of energy generation after starvation. However, regulation of gluconeogenesis through Nur77 and blood glucose level (Kim et al., 2014) were not significantly changed in the TIS21-KO mice

compared with that of WT after 24 h fasting (data not shown). The collective data imply the role of TIS21 expression in maintaining energy level under stressful conditions by regulating fatty acid oxidation in the liver.

Cathepsin E (Ctse) is as a member of the aspartate endopeptidase localized in the late endosome or plasma membrane, and mostly within antigen-presenting cells (Yamamoto et al., 2012). It is highly expressed in gastrointestinal mucosa and lymphoid organs including the fetal liver, but obviously not in adult liver (Chlabicz et al., 2011; Kageyama et al., 1998). Presently, *Ctse* expression was very high in adult liver as well as lymphoid organs of TIS21-KO mice (Fig. 4C). Therefore, we can suggest a significant role of the TIS21 gene in regulating *Ctse* expression in lymphoid organs and adult liver during starvation. Although we cannot suggest a reason yet, a plausible mechanism is that activation of cytochrome P450 regulating genes may produce ligands for constitutive androstane receptor/retinoid X receptor heterodimer (CAR/RXRα) (Page et al., 2007) which may stimulate *Ctse* expression in TIS21-KO mice. How does TIS21$^{/BTG2/PC3}$ regulate PPARα signaling under fasting condition? It has been reported that PPARα shares RXRα as a heterodimeric nuclear receptor complex and TIS21 binds to nuclear receptor *via* two LXXLL motifs (Hu et al., 2011; Passeri et al., 2006), which may indicate a possible clue in the regulation of *Ctse* and β-oxidative genes at the downstream of PPARα. Moreover, PGC1α, a co-activator of PPARα, expression was also downregulated in the TIS21-KO mice. Thus TIS21 knockout-mediated downregulation of PPARα activity and *Ctse* expression need to further investigate during fasting.

On the other hand, expression of glutaredoxin 2 was also significantly reduced in liver of TIS21-KO mice compared to WT mice (Fig. 4B), and the focal fatty change in livers of TIS21-KO mice (Supplementary Fig. S4 and Supplementary Table S2) may reflect deficit of anti-oxidative capacity during overnight fasting. The assumption can be supported by previous reports that the expression of TIS21$^{/BTG2}$ downregulates reactive oxygen species (ROS) generation (Choi and Lim, 2013; Lim et al., 2012) , that glutaredoxin 2 plays a protective role against hydrogen peroxide-induced damage and that its loss sensitizes cells to oxidative stress and apoptosis (Wu et al., 2010). In addition, TIS21 stimulates manganese superoxide dismutase (SOD2) transcription by nuclear factor-kappa B *via* crosstalk with phosphoinositol-3-kinase-AKT1 activation (Sundaramoorthy et al., 2013).

Taken together, the data indicate that the expression of the TIS21 gene protects cells and tissues from the fasting-induced ROS generation. In conclusion, we strongly suggest that TIS21$^{/BTG2}$ as an essential gene for anti-oxidative role against ROS and for regulation of fatty acid β-oxidation under stressful conditions, such as fasting and starvation.

Note: Supplementary information is available on the Molecules and Cells website (www.molcells.org).

ACKNOWLEDGMENTS

This work was supported by the National Research Foundation (NRF) grant funded by the Korean government (MSIP; No.2016R1A2B4006466).

REFERENCES

Bradbury, A., Possenti, R., Shooter, E.M., and Tirone, F. (1991). Molecular cloning of PC3, a putatively secreted protein whose mRNA is induced by nerve growth factor and depolarization. Proc. Natl. Acad. Sci. USA *88*, 3353-3357.

Cahill Jr, G.F. (2006). Fuel metabolism in starvation. Annu. Rev. Nutr. *26*, 1-22.

Chlabicz, M., Gacko, M., Worowska, A., and Łapiński, R. (2011). Cathepsin E (EC 3.4. 23.34)—a review. Folia Histochem. Cytobiol. *49*, 547-557.

Choi, J.-A., and Lim, I.K. (2013). TIS21/BTG2 inhibits invadopodia formation by downregulating reactive oxygen species level in MDA-MB-231 cells. J. Cancer Res. Clin. Oncol. *139*, 1657-1665.

Choi, J., Jung, Y., Kim, J., Kim, H., and Lim, I. (2016). Inhibition of breast cancer invasion by TIS21/BTG2/Pc3-Akt1-Sp1-Nox4 pathway targeting actin nucleators, mDia genes. Oncogene *35*, 83.

Fletcher, B., Lim, R., Varnum, B., Kujubu, D., Koski, R., and Herschman, H. (1991). Structure and expression of TIS21, a primary response gene induced by growth factors and tumor promoters. J. Biol. Chem. *266*, 14511-14518.

Folch, J., Lees, M., and Sloane-Stanley, G. (1957). A simple method for the isolation and purification of total lipids from animal tissues. J. Biol. Chem. *226*, 497-509.

Hakvoort, T.B., Moerland, P.D., Frijters, R., Sokolović, A., Labruyère, W.T., Vermeulen, J.L., van Themaat, E.V.L., Breit, T.M., Wittink, F.R., and van Kampen, A.H. (2011). Interorgan coordination of the murine adaptive response to fasting. J. Biol. Chem. *286*, 16332-16343.

Hu, X.-D., Meng, Q.-H., Xu, J.-Y., Jiao, Y., Ge, C.-M., Jacob, A., Wang, P., Rosen, E.M., and Fan, S. (2011). BTG2 is an LXXLL-dependent co-repressor for androgen receptor transcriptional activity. Biochem. Biophys. Res. Commun. *404*, 903-909.

Huang, D.W., Sherman, B.T., and Lempicki, R.A. (2008). Bioinformatics enrichment tools: paths toward the comprehensive functional analysis of large gene lists. Nucleic Acids Res. *37*, 1-13.

Huang, D.W., Sherman, B.T., and Lempicki, R.A. (2009). Systematic and integrative analysis of large gene lists using DAVID bioinformatics resources. Nat. Protocols *4*, 44.

Hwang, S.-L., Kwon, O., Lee, S.J., Roh, S.-S., Kim, Y.D., and Choi, J.H. (2012). B-cell translocation gene-2 increases hepatic gluconeogenesis via induction of CREB. Biochem. Biophys. Res. Commun. *427*, 801-805.

Kageyama, T., Tatematsu, M., Ichinose, M., Yahagi, N., Miki, K., Moriyama, A., and Yonezawa, S. (1998). Development-dependent expression of cathepsins d and e in various rat tissues, with special reference to the high expression of cathepsin e in fetal liver. Zool. Sci. *15*, 517-523.

Kanehisa, M., and Goto, S. (2000). KEGG: kyoto encyclopedia of genes and genomes. Nucleic Acids Res. *28*, 27-30.

Kanehisa, M., Sato, Y., Kawashima, M., Furumichi, M., and Tanabe, M. (2016). KEGG as a reference resource for gene and protein annotation. Nucleic Acids Res. *44*, D457-D462.

Kim, B.C., Ryu, M.S., Oh, S.P., and Lim, I.K. (2008). TIS21/BTG2 negatively regulates estradiol-stimulated expansion of hematopoietic stem cells by derepressing Akt phosphorylation and inhibiting mTOR signal transduction. Stem Cells *26*, 2339-2348.

Kim, Y.-D., Im, S.-S., Oh, B.-C., Bae, J.-H., and Song, D.-K. (2014). B-cell Translocation Gene 2 regulates hepatic glucose homeostasis via induction of orphan nuclear receptor Nur77 in diabetic mouse model. Diabetes *63*, 1870-1880

Komatsu, M., Waguri, S., Ueno, T., Iwata, J., Murata, S., Tanida, I., Ezaki, J., Mizushima, N., Ohsumi, Y., and Uchiyama, Y. (2005). Impairment of starvation-induced and constitutive autophagy in Atg7-deficient mice. J. Cell Biol. *169*, 425-434.

Lee, Y.-H., Kim, H.-J., Lee, W.-Y., Kim, M.-J., Tark, D.-S., Cho, I.-S., and Sohn, H.-J. (2012). Gene expression profile of a persistently chronic wasting disease (CWD) prion-infected RK13 cell line. J. Prev. Veterinary Med. *36*, 186-195.

Lee, J.M., Wagner, M., Xiao, R., Kim, K.H., Feng, D., Lazar, M.A., and Moore, D.D. (2014). Nutrient-sensing nuclear receptors coordinate autophagy. Nature *516*, 112-115.

Li, C., Yu, S., Zhong, X., Wu, J., and Li, X. (2012). Transcriptome comparison between fetal and adult mouse livers: implications for circadian clock mechanisms. PloS one *7*, e31292.

Lim, I.K. (2006). TIS21/BTG2/PC3 as a link between ageing and cancer: cell cycle regulator and endogenous cell death molecule. J. Cancer Res. Clin. Oncol. *132*, 417-426.

Lim, I.K., Lee, M.S., Lee, S.H., Kim, N.K., Jou, I., Seo, J.-S., and Park, S.C. (1995). Differential expression of TIS21 and TIS1 genes in the various organs of Balb/c mice, thymic carcinoma tissues and human cancer cell lines. J. Cancer Res. Clin. Oncol. *121*, 279-284.

Lim, S.-K., Choi, Y.W., Lim, I.K., and Park, T.J. (2012). BTG2 suppresses cancer cell migration through inhibition of Src-FAK signaling by downregulation of reactive oxygen species generation in mitochondria. Clin. Exp. Metastasis *29*, 901-913.

Mao, B., Zhang, Z., and Wang, G. (2015). BTG2: A rising star of tumor suppressors. Int. J. Oncol. *46*, 459-464.

Mizushima, N., Yamamoto, A., Matsui, M., Yoshimori, T., and Ohsumi, Y. (2004). In vivo analysis of autophagy in response to nutrient starvation using transgenic mice expressing a fluorescent autophagosome marker. Mol. Biol. Cell *15*, 1101-1111.

Mootha, V.K., Lindgren, C.M., Eriksson, K.-F., Subramanian, A., Sihag, S., Lehar, J., Puigserver, P., Carlsson, E., Ridderstråle, M., and Laurila, E. (2003). PGC-1α-responsive genes involved in oxidative phosphorylation are coordinately downregulated in human diabetes. Nat. Genet. *34*, 267-273.

Newberry, E.P., Xie, Y., Kennedy, S., Han, X., Buhman, K.K., Luo, J., Gross, R.W., and Davidson, N.O. (2003). Decreased hepatic triglyceride accumulation and altered fatty acid uptake in mice with deletion of the liver fatty acid-binding protein gene. J. Biol. Chem. *278*, 51664-51672.

Page, J.L., Strom, S.C., and Omiecinski, C.J. (2007). Regulation of the human cathepsin E gene by the constitutive androstane receptor. Arch. Biochem. Biophys. *467*, 132-138.

Park, S., Lee, Y.J., Lee, H.-J., Seki, T., Hong, K.-H., Park, J., Beppu, H., Lim, I.K., Yoon, J.-W., and Li, E. (2004). B-cell translocation gene 2 (Btg2) regulates vertebral patterning by modulating bone morphogenetic protein/smad signaling. Mol. Cell. Biol. *24*, 10256-10262.

Park, T.J., Kim, J.Y., Oh, S.P., Kang, S.Y., Kim, B.W., Wang, H.J., Song, K.Y., Kim, H.C., and Lim, I.K. (2008). TIS21 negatively regulates hepatocarcinogenesis by disruption of cyclin B1-Forkhead box M1 regulation loop. Hepatology *47*, 1533-1543.

Passeri, D., Marcucci, A., Rizzo, G., Billi, M., Panigada, M., Leonardi, L., Tirone, F., and Grignani, F. (2006). Btg2 enhances retinoic acid-induced differentiation by modulating histone H4 methylation and acetylation. Mol. Cell. Biol. *26*, 5023-5032.

Rabinowitz, J.D., and White, E. (2010). Autophagy and metabolism. Science *330*, 1344-1348.

Rakhshandehroo, M., Knoch, B., Müller, M., and Kersten, S. (2010). Peroxisome proliferator-activated receptor alpha target genes. PPAR Res. *2010*.

Rouault, J.P., Falette, N., Guehenneux, F., Guillot, C., Rimokh, R., Wang, Q., Berthet, C., Moyret-Lalle, C., Savatier, P., Pain, B., et al. (1996). Identification of BTG2, an antiproliferative p53-dependent component of the DNA damage cellular response pathway. Nat. Genet. *14*, 482-486.

Schupp, M., Chen, F., Briggs, E.R., Rao, S., Pelzmann, H.J., Pessentheiner, A.R., Bogner-Strauss, J.G., Lazar, M.A., Baldwin, D., and Prokesch, A. (2013). Metabolite and transcriptome analysis during fasting suggest a role for the p53-Ddit4 axis in major metabolic tissues. BMC Genomics *14*, 758.

Shannon, P., Markiel, A., Ozier, O., Baliga, N.S., Wang, J.T., Ramage, D., Amin, N., Schwikowski, B., and Ideker, T. (2003). Cytoscape: a software environment for integrated models of biomolecular interaction networks. Genome Res. *13*, 2498-2504.

Subramanian, A., Tamayo, P., Mootha, V.K., Mukherjee, S., Ebert, B.L., Gillette, M.A., Paulovich, A., Pomeroy, S.L., Golub, T.R., and Lander, E.S. (2005). Gene set enrichment analysis: a knowledge-based approach for interpreting genome-wide expression profiles. Proc. Natl. Acad. Sci. USA *102*, 15545-15550.

Sundaramoorthy, S., Ryu, M.S., and Lim, I.K. (2013). B-cell translocation gene 2 mediates crosstalk between PI3K/Akt1 and NFκB pathways which enhances transcription of MnSOD by accelerating IκBα degradation in normal and cancer cells. Cell Commun. Signal. *11*, 69.

Terra, R., Luo, H., Qiao, X., and Wu, J. (2008). Tissue-specific expression of B-cell translocation gene 2 (BTG2) and its function in T-cell immune responses in a transgenic mouse model. Int. Immunol. *20*, 317-326.

Wu, H., Xing, K., and Lou, M.F. (2010). Glutaredoxin 2 prevents H2O2-induced cell apoptosis by protecting complex I activity in the mitochondria. Biochim. Biophys. Acta -Bioenergetics *1797*, 1705-1715.

Yamamoto, K., Kawakubo, T., Yasukochi, A., and Tsukuba, T. (2012). Emerging roles of cathepsin E in host defense mechanisms. Biochim. Biophys. Acta -Bioenergetics *1824*, 105-112.

Zhang, F., Xu, X., Zhou, B., He, Z., and Zhai, Q. (2011). Gene expression profile change and associated physiological and pathological effects in mouse liver induced by fasting and refeeding. PloS one *6*, e27553.